Growth of vortical disturbances entrained in the entrance region of a circular pipe - supplementary material

Pierre Ricco[1]† and Claudia Alvarenga[1,2]

[1]Department of Mechanical Engineering, The University of Sheffield, S1 3JD Sheffield, United Kingdom

[2]Department of Fluid Dynamics, A*Star Institute of High Performance Computing, Singapore

(Received xx; revised xx; accepted xx)

This supplementary material presents further analysis that is used in the paper and additional theoretical and numerical results.

S1. Numerical procedures

The base-flow boundary-layer and continuity equations (2.8)-(2.9), supplemented by the mass conservation law, are discretized according to a scheme that is an improved version of that used by Hornbeck (1964). The base-flow streamwise velocity and pressure fields are computed simultaneously and the base-flow radial velocity is computed a posteriori through the continuity equation. A difference from Hornbeck (1964) regards the treatment of the nonlinear convective terms in the base-flow x-momentum equation (2.9). In their paper, these terms are linearized, i.e., the values at the previous x locations are used in the nonlinear terms. Here, we instead use a predictor-corrector method for the computation of the convective terms at step $\overline{n}$. In the predictor step $\overline{n}-1$, an initial approximation of the streamwise velocity and pressure fields is calculated via the linearized discretized equations as in Hornbeck (1964). In the corrector step, new values of $U^{\overline{n}}$ and $P^{\overline{n}}$ are computed, using $U^{\overline{n}-1}$ and $P^{\overline{n}-1}$ in the discretization of the convective terms instead of those at the previous streamwise location. This procedure is repeated iteratively until convergence is reached. The convergence criterion is based on the radial velocity gradient at the wall, $\partial U/\partial r|_{r=R}$. The asymptotic composite solution derived in §3.1 is used as initial condition at small $\overline{x}$ values.

The perturbation equations (2.11)-(2.12) are discretized using backward and central finite-difference schemes in $\overline{x}$ and r, respectively. The degree of the radial velocity equation (2.11) is reduced from fourth to second by defining the radial second derivative of $\overline{u}_r$ as a new variable. The resulting system is written in the form of a block tridiagonal matrix and solved at each $\overline{x}$ by the Thomas algorithm (Cebeci 2002). The asymptotic composite solution given in §3.2 is used as initial condition at small $\overline{x}$ values. At each $\overline{x}$ location the behaviour of the velocity field as the pipe axis is approached is checked against the asymptotic results of Lewis & Bellan (1990), discussed in §S3.2.

† Email address for correspondence: p.ricco@sheffield.ac.uk

S2. Boundary-region equations

We herein derive the final form of the boundary-region equations. In expanded form, equations (2.3) and (2.4) read

$$\frac{1}{r}\frac{\partial}{\partial r}\left(ru_r\right)+\frac{1}{r}\frac{\partial u_\theta}{\partial\theta}+\frac{\partial u_x}{\partial x}=0, \tag{S2.1}$$

$$\begin{aligned}&\frac{\partial u_x}{\partial t}+u_x\frac{\partial u_x}{\partial x}+u_r\frac{\partial u_x}{\partial r}+\frac{u_\theta}{r}\frac{\partial u_x}{\partial\theta}=-\frac{\partial p}{\partial x}+\frac{1}{Re_\lambda}\frac{\partial^2 u_x}{\partial x^2}+\\&\frac{1}{rRe_\lambda}\frac{\partial}{\partial r}\left(r\frac{\partial u_x}{\partial r}\right)+\frac{1}{r^2Re_\lambda}\frac{\partial^2 u_x}{\partial\theta^2},\end{aligned} \tag{S2.2}$$

$$\begin{aligned}&\frac{\partial u_r}{\partial t}+u_x\frac{\partial u_r}{\partial x}+u_r\frac{\partial u_r}{\partial r}+\frac{u_\theta}{r}\frac{\partial u_r}{\partial\theta}-\frac{u_\theta^2}{r}=-\frac{\partial p}{\partial r}+\frac{1}{Re_\lambda}\frac{\partial^2 u_r}{\partial x^2}+\\&\frac{1}{Re_\lambda}\frac{\partial}{\partial r}\left[\frac{1}{r}\frac{\partial(ru_r)}{\partial r}\right]+\frac{1}{r^2Re_\lambda}\frac{\partial^2 u_r}{\partial\theta^2}-\frac{2}{r^2Re_\lambda}\frac{\partial u_\theta}{\partial\theta},\end{aligned} \tag{S2.3}$$

$$\begin{aligned}&\frac{\partial u_\theta}{\partial t}+u_x\frac{\partial u_\theta}{\partial x}+u_r\frac{\partial u_\theta}{\partial r}+\frac{u_\theta}{r}\frac{\partial u_\theta}{\partial\theta}+\frac{u_ru_\theta}{r}=-\frac{1}{r}\frac{\partial p}{\partial\theta}+\frac{1}{Re_\lambda}\frac{\partial^2 u_\theta}{\partial x^2}+\\&\frac{1}{Re_\lambda}\frac{\partial}{\partial r}\left[\frac{1}{r}\frac{\partial(ru_\theta)}{\partial r}\right]+\frac{1}{r^2Re_\lambda}\frac{\partial^2 u_\theta}{\partial\theta^2}+\frac{2}{r^2Re_\lambda}\frac{\partial u_r}{\partial\theta}.\end{aligned} \tag{S2.4}$$

The substitution of (2.6)-(2.7) into (S2.1)-(S2.4) leads to the base-flow equations (2.8)-(2.10) by collecting $\mathcal{O}(1)$ terms in the limits $k_x, Re_\lambda^{-1}\ll 1$ and $\mathcal{F}=\mathcal{O}(1)$. By collecting $\mathcal{O}(\varepsilon)$ terms, the boundary-region equations for the perturbation flow are found,

$$\frac{\partial\overline{u}_x}{\partial\overline{x}}+\frac{\overline{u}_r}{r}+\frac{\partial\overline{u}_r}{\partial r}+\frac{\overline{u}_\theta}{r}=0, \tag{S2.5}$$

$$\left(-i+\frac{\partial U}{\partial\overline{x}}+\frac{m^2}{\mathcal{F}r^2}\right)\overline{u}_x+U\frac{\partial\overline{u}_x}{\partial\overline{x}}+\left(V-\frac{1}{\mathcal{F}r}\right)\frac{\partial\overline{u}_x}{\partial r}+\frac{\partial U}{\partial r}\overline{u}_r-\frac{1}{\mathcal{F}}\frac{\partial^2\overline{u}_x}{\partial r^2}=0, \tag{S2.6}$$

$$\begin{aligned}&\left(-i+\frac{\partial V}{\partial r}+\frac{m^2+1}{\mathcal{F}r^2}\right)\overline{u}_r+U\frac{\partial\overline{u}_r}{\partial\overline{x}}+\left(V-\frac{1}{\mathcal{F}r}\right)\frac{\partial\overline{u}_r}{\partial r}+\frac{\partial V}{\partial\overline{x}}\overline{u}_x+\\&\frac{2}{\mathcal{F}r^2}\overline{u}_\theta+\frac{1}{\mathcal{F}}\frac{\partial\overline{p}}{\partial r}-\frac{1}{\mathcal{F}}\frac{\partial^2\overline{u}_r}{\partial r^2}=0,\end{aligned} \tag{S2.7}$$

$$\left(-i+\frac{V}{r}+\frac{m^2+1}{\mathcal{F}r^2}\right)\overline{u}_\theta+U\frac{\partial\overline{u}_\theta}{\partial\overline{x}}+\left(V-\frac{1}{\mathcal{F}r}\right)\frac{\partial\overline{u}_\theta}{\partial r}+\frac{2m^2}{\mathcal{F}r^2}\overline{u}_r-\frac{m^2}{\mathcal{F}r}\overline{p}-\frac{1}{\mathcal{F}}\frac{\partial^2\overline{u}_\theta}{\partial r^2}=0. \tag{S2.8}$$

Equations (S2.5)-(S2.8) are also satisfied by $\left\{\overline{u}_x^{(0)},\overline{u}_r^{(0)},\overline{u}_\theta^{(0)},\overline{p}^{(0)}\right\}$. The pressure and the spanwise velocity component are eliminated from (S2.7) and (S2.8) to find (2.11) and (2.12).

S3. Conditions at the pipe axis

In the cylindrical geometry, the pipe axis is a singularity in the equations of motion, but the velocity vector and the pressure must be regular there. Constraints on these

quantities must thus be satisfied, which leads to a specific behaviour of the Bessel-Fourier coefficients as the axis is approached and to the boundary conditions at the axis. We obtain the boundary conditions following the study of Lewis & Bellan (1990), discuss the regularity conditions found by Batchelor & Gill (1962) and Khorrami *et al.* (1989), and further analyze the problem according to Tuckerman (1989).

S3.1. *Boundary conditions at the pipe axis*

The boundary conditions for the perturbation flow at $r = 0$ are given in (2.28)-(2.30). The boundary conditions (2.28) for $m = 1$ involve the azimuthal velocity $\overline{u}_\theta$ and therefore (2.11)-(2.12) are solved together with the continuity equation (S2.5). For $m = 2$, there is no need to solve for the continuity equation; as $\overline{u}_r''$ is used as a new independent variable in the numerical solver, the last boundary conditions in (2.29) is replaced by $\overline{u}_r'' = 0$ because $\overline{u}_r$ grows linearly with r from the pipe axis at leading order (Lewis & Bellan 1990).

S3.2. *Symmetry and regularity at the pipe axis*

The radial behaviour of the velocity components found in Lewis & Bellan (1990) allows us to obtain the boundary conditions at $r = 0$ used to solve (2.11)-(2.12). Information on the velocity field can be inferred by imposing symmetry and regularity at the axis (Lewis & Bellan 1990). The streamwise velocity behaves as a scalar, i.e., $u_x \sim \hat{\psi}_m r^m e^{im\theta}$ as $r \to 0$. Lewis & Bellan (1990) explain that the radial and azimuthal velocity components do not behave as scalars at the axis and, by imposing regularity, they find $u_{r,m} \sim \hat{\lambda}_m r^{m-1} e^{im\theta}$, $u_{\theta,m} \sim i\hat{\lambda}_m r^{m-1} e^{im\theta}$ and $u_{r,m} + iu_{\theta,m} \to 0$ as $r \to 0$. When the vector is solenoidal, the last condition is verified exactly at $r = 0$. Our oncoming disturbance (2.1) and the solutions in region I, (3.19)-(3.21) and (3.31), all satisfy these conditions. For the gust disturbance, $\hat{\psi}_m = \hat{u}^\infty_{x,mn}(\xi_{mn}/4R)^m/\Gamma(m+1)$ and $\hat{\lambda}_m = \hat{u}^\infty_{r,mn}(\xi_{mn}/2R)^{m-1}/[2^m\Gamma(m+1)]$, while, in region I, we find $\hat{\lambda}_m = -2\hat{u}^\infty_{r,mn} J_m(\xi_{mn}/2) R^{1-m} e^{i\overline{x}}/\xi_{mn}$ for the leading-order components and $\hat{\lambda}_m = -\beta\hat{u}^\infty_{x,mn} J_m(\xi_{mn}/2) R^{1-m}/[2(2\overline{x}k_x R_\lambda)^{1/2}]$ for the next-order components.

Tuckerman (1989) further elucidates that, in order to guarantee regularity at the pipe axis, two conditions must be met when the velocity field Fourier-expands as $\hat{u} \sim r^{\hat{j}} e^{im\theta}$ when $r \to 0$, which is the behaviour that occurs for our free-stream disturbance (2.1) and in region I. For the streamwise component, i) $\hat{j} + m$ must be even and ii) $\hat{j} \geqslant m$, while, for the radial and azimuthal components, i) $\hat{j} + m$ must be odd and ii) $\hat{j} \geqslant \min\{m-1, 2\}$. The number 2 in the last expression arises from imposing regularity on the Laplacian of the velocity vector. This condition is not strictly necessary for our inviscid free-stream and region-I disturbances, but we keep this restriction because these perturbations are utilized as initial conditions for the viscous boundary-region equations. In the last expression, Tuckerman (1989) also finds that $m+1$ must be considered together with $m-1$ for the combination $u_{r,m} + iu_{\theta,m}$ (refer to her (5.4)), but in our specific case $u_{r,m} + iu_{\theta,m} \to 0$ because of continuity and therefore it is sufficient to consider $m-1$. The boundary conditions are fully consistent with Tuckerman (1989)'s conditions. The asymptotic behaviours found by Lewis & Bellan (1990) all satisfy Tuckerman (1989)'s conditions and so do our oncoming disturbances and region-I solutions, as shown by using the exponent $\hat{j}$ of the Bessel-function expansions given by Abramowitz & Stegun (1972).

S3.3. *Independence of the velocity vector from the azimuthal angle at the pipe axis*

Batchelor & Gill (1962) and Khorrami *et al.* (1989) explain that the velocity field must be independent of the azimuthal angle as the pipe axis is approached, i.e., $\lim_{r\to 0} \partial\mathbf{u}/\partial\theta = 0$. This limit translates to the conditions i) $\partial u_x/\partial\theta$=0, ii) $\partial u_r/\partial\theta - u_\theta$=0, iii) $u_r + \partial u_\theta/\partial\theta$=0. These conditions are satisfied by the free-stream gust (2.1), the solutions in region I found in §3.2.1, and our boundary conditions at the pipe axis.

For the free-stream gust, it is convenient to use the asymptotic expression $J_m(\overline{r}) \sim (\overline{r}/2)^m/\Gamma(m+1)$ for $\overline{r} \ll 1$. Condition i) is satisfied when $m \neq 0$ because $J_m(0) = 0$ in these cases. Condition ii) is satisfied when $m = 0$ because $J_0'(0) = 0$, when $m = 1$ because the continuity condition (2.2) applies, and when $m > 1$ because both terms of the solutions are $\sim r^{m-1}$. Condition iii) is satisfied when $m = 0$ if we set $\hat{u}_{r,0n} = 0$, and when $m > 0$ for the same reasons as for condition ii). Condition (2.2) further agrees with the continuity check in equation (20) in Khorrami *et al.* (1989).

The leading-order solutions in region I, (3.22)-(3.24), satisfy the three conditions. Condition i) is satisfied because of (3.22a) and conditions ii) and iii) are satisfied for the same reasons as the gust velocity components because the potential (3.18) leads to velocity components that have the same asymptotic behaviour of the gust components as $r \to 0$. The solutions in region I arising from the potential (3.18) satisfy condition i), while conditions ii) and iii) are satisfied when $m = 0$ if $\hat{u}_{x,0n} = 0$, when $m = 1$ if $\hat{u}_{x,1n} = 0$, and always when $m > 1$ because the solution is $\sim r^{m-1}$.

The boundary conditions at the pipe axis can be found by imposing conditions i), ii), and iii) on (2.7). They apply to both $\overline{u}_x, \overline{u}_r, \overline{u}_\theta$ and $\overline{u}_x^{(0)}, \overline{u}_r^{(0)}, \overline{u}_\theta^{(0)}$. When $m > 0$ condition i) leads to $\overline{u}_x = 0$, condition ii) gives $m^2\overline{u}_r + \overline{u}_\theta = 0$, and condition iii) gives $\overline{u}_r + \overline{u}_\theta = 0$. It follows that $\overline{u}_x = \overline{u}_r = \overline{u}_\theta = 0$ at $r = 0$ when $m > 1$. Similar to Khorrami *et al.* (1989), linearly dependent conditions occur when $m = 1$ and thus $\overline{u}_r + \overline{u}_\theta = 0$ in this case. These conditions are the same as those found following Lewis & Bellan (1990). L'Hôpital's rule is used on the continuity equation to find $2\partial\overline{u}_r/\partial r + \partial\overline{u}_\theta/\partial r = 0$ at $r = 0$ for every m (Khorrami *et al.* 1989). This condition is simplified to $\partial\overline{u}_r/\partial r = 0$ when $m \neq 2$ by use of the radial dependence found by Lewis & Bellan (1990).

S4. Negligible near-wall curvature effects

We demonstrate that the curvatures effects are negligible near the pipe entrance and near the wall (region II) when $Re_\lambda \gg 1$. This limit allows simplifying the Navier-Stokes equations in cylindrical coordinates (S2.1)-(S2.4) to the boundary-layer equations in Cartesian coordinates for both the base flow and the perturbation flow in the proximity of the wall. It follows that in region II the inner velocities $\{u_{x,in}, u_{r,in}, u_{\theta,in}\}$ are given by the Blasius solution for the base flow and by the solutions (4.13) on page 177 of Leib *et al.* (1999) for the boundary-layer perturbation flow.

The boundary-layer thickness is asymptotically smaller than the pipe radius, i.e., $\delta/R \ll 1$, which follows from $Re_\lambda \gg 1$. Since $y = R - r$, where y is measured from the pipe wall toward the pipe axis, we insert the following changes in (S2.1)-(S2.4): $r \to R$, $\partial/\partial r \to -\partial/\partial y$, $\partial^2/\partial r^2 \to \partial^2/\partial y^2$, $\theta \to z/R$, and $\{u_x, u_r, u_\theta\} \to \{u_{x,in}, -u_{r,in}, u_{z,in}\}$. The azimuthal modulation of the perturbation changes as $m\theta \to k_z z$, where $k_z = 2\pi$, because $m = 2\pi R = \mathcal{O}(1)$. The continuity equation (S2.1) immediately reduces to the Cartesian form. Besides the x-diffusion term that is negligible under the usual large-Re_λ assumption, the x-momentum equation (S2.2) has three viscous terms: i) $(RRe_\lambda)^{-1}\partial u_{x,in}/\partial y$, ii) $Re_\lambda^{-1}\partial^2 u_{x,in}/\partial y^2$, and iii) $Re_\lambda^{-1}\partial^2 u_{x,in}/\partial z^2$. Term ii) is asymptotically larger than the others because the near-wall scaling $y/\delta = \mathcal{O}(1)$

leads to $\delta \ll R$. The θ-momentum equation (S2.4) has one extra convective term and three viscous terms: i) $-u_{y,in}u_{z,in}/R$, ii) $Re_\lambda^{-1}\partial^2 u_{x,in}/\partial y^2$, iii) $Re_\lambda^{-1}\partial^2 u_{x,in}/\partial z^2$, and iv) $-2(RRe_\lambda)^{-1}\partial u_{y,in}/\partial z$. Like for the x-momentum equation, term ii) is asymptotically larger than the others because $\delta \ll R$. The y-momentum equation reduces to the vanishing wall-normal pressure gradient. The Cartesian boundary-layer equations are recovered, where the spanwise viscous effects are identically zero for the base flow and negligible for the perturbation flow.

S5. Inviscid base-flow Stokes streamfunction ψ_2

Equation (3.7) is solved by using the complex Fourier transform along x, whose inverse is

$$\psi_2(x,r) = \frac{1}{\sqrt{2\pi}} \int_{-\infty+i\gamma}^{+\infty+i\gamma} \hat{\psi}_2(\zeta,r) e^{i\zeta x} \mathrm{d}\zeta, \tag{S5.1}$$

where the use of $\gamma \in \mathbb{R} < 0$ is required to render $\sqrt{x}e^{\gamma x}$ absolutely integrable when $x > 0$. This integration path is necessary to define the complex Fourier transform of the boundary condition (3.8a). The function $\hat{\psi}_2$ satisfies $r\hat{\psi}_2'' - \hat{\psi}_2' - r\zeta^2\hat{\psi}_2 = 0$. The bounded solution that satisfies the boundary condition (3.8c) is $\hat{\psi}_2 = k_1(\zeta) r I_1(\zeta r)$ because the other solution proportional to the unbounded modified Bessel function of the second kind K_1 must vanish (the Frobenius method shows that it is not multiplied by r). By substituting the solution of $\hat{\psi}_2$ into (S5.1) and using the complex Fourier transform of (3.8a) and (3.8b), we find that

$$k_1(\zeta) = \frac{\beta\sqrt{2}}{I_1(\zeta R)} \int_0^\infty \sqrt{\xi} e^{-i\xi\zeta} \mathrm{d}\xi, \tag{S5.2}$$

where $\Im(\zeta) < 0$ for the integral in (S5.2) to be defined. The solution to (3.7) is

$$\psi_2(x,r) = \frac{\beta r}{\pi\sqrt{2}} \int_{-\infty+i\gamma}^{+\infty+i\gamma} \frac{I_1(\zeta r) e^{i\zeta x}}{I_1(\zeta R)} \int_0^\infty \sqrt{\xi} e^{-i\xi\zeta} \mathrm{d}\xi \mathrm{d}\zeta. \tag{S5.3}$$

The second integral, i.e., the complex Laplace transform which exists because $\gamma < 0$ (refer to page 401 of Dettman (1965)), leads to the final solution (3.11).

It is immediate to verify that (3.11) satisfies the boundary condition at the pipe axis, (3.8c). To verify that (3.8a) for $x > 0$ and (3.8b) for $x < 0$ are satisfied, the contour paths in the left and the right graphs of figure S1, are used, respectively. For both contour paths, the residue is zero because no poles are contained within the paths and the integral along the line l ($\Im(\zeta) = \gamma$) is (3.11) with $r = R$, i.e., the modified Bessel functions cancel out. In the left graph of figure S1, the integrals along l_1 and l_2 cancel out and the integrals along the arcs a_1 and a_2 tend to zero as the radius of the arcs R_a increases. Upon setting $\zeta = i\gamma + R_a e^{i\theta}$, $0 < \theta < \pi$, we note $|e^{i\zeta x}| = |e^{-\gamma x} e^{ixR_a(\cos\theta + i\sin\theta)}| = e^{-\gamma x} e^{-xR_a\sin\theta} \leqslant e^{-\gamma x}$, which justifies the choice of the arcs in that θ range and implies that

$$\int_{a_1,a_2} \frac{e^{i\zeta x}}{\zeta^{3/2}} \mathrm{d}\zeta \leqslant \frac{e^{-\gamma x}\pi R_a}{(R_a - \gamma)^{3/2}} \to 0 \quad \text{as} \quad R_a \to \infty. \tag{S5.4}$$

It follows that (3.11) with $r = R$ and $x > 0$ is equal to the opposite of the integral along the circle c in the left graph of figure S1. By changing the variable $\overline{\zeta} = i\zeta x$ in the integral along c, one finds the Hankel contour integral representation of the reciprocal of the gamma function, as shown on page 197 of Dettman (1965), which leads to (3.8a). When $x < 0$, (3.8b) follows immediately because the integral along the arc a_3 in the

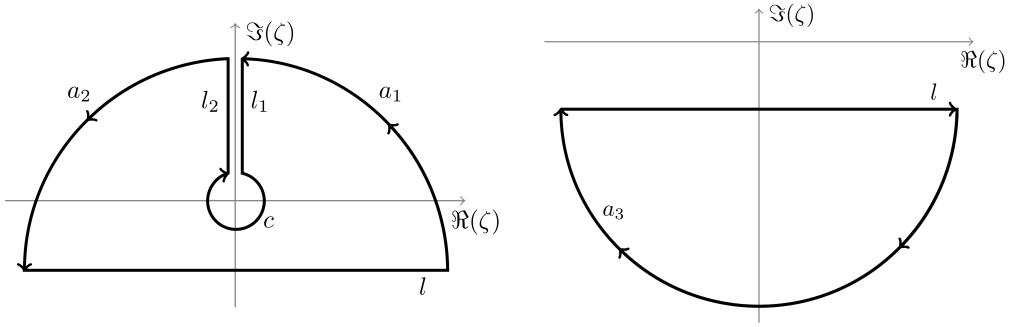

Figure S1: Contour paths of integration to verify that the solution (3.11) satisfies the boundary conditions (3.8a) ($x > 0$, left graph) and (3.8b) ($x < 0$, right graph).

right graph of figure S1 vanishes as R_a increases, following an argument analogous to the integrals along a_1 and a_2, the difference lying in the range $\pi < \theta < 2\pi$.

S6. Leading-order perturbation potential in region I

The solution to (3.15) that satisfies the boundary conditions (3.16) can be obtained by separation of variables when $x \gg 1$, i.e., $\phi = \hat{\phi}(r) \exp[ik_x(x-t) + im\theta]$, where the x dependence is found by matching with the gust (2.1). The quantity $\hat{\phi}(r)$ satisfies the modified Bessel equation (3.17) and is equal to

$$\hat{\phi}(r) = -\frac{\hat{u}^{\infty}_{r,mn} J_m(\xi_{mn}/2) I_m(k_x r)}{k_x R I'_m(k_x R)} = \mathcal{O}(1), \tag{S6.1}$$

where I_m is the modified Bessel function of order m. As $k_x \ll 1$, the asymptotic behaviour of the modified Bessel function for small argument, i.e., $I_m(k_x r) \sim \Gamma(m+1)^{-1} (k_x r/2)^m$(Abramowitz & Stegun 1972), is substituted into (S6.1) to find

$$\hat{\phi}(r) = -\frac{2R\hat{u}^{\infty}_{r,mn} J_m(\xi_{mn}/2)}{m\xi_{mn}} \left(\frac{r}{R}\right)^m, \tag{S6.2}$$

from which (3.18) is found. Solution (S6.2) is also found by solving the Euler differential equation that arises by neglecting the term proportional to $k_x^2 \ll 1$ in (3.15).

REFERENCES

Abramowitz, M. & Stegun, I.A. 1972 *Handbook of Mathematical Functions*, Tenth edn. Dover, New York.

Batchelor, G.K. & Gill, A.E. 1962 Analysis of the stability of axisymmetric jets. *J. Fluid Mech.* **14** (4), 529–551.

Cebeci, T. 2002 *Convective Heat Transfer*. Springer-Verlag, Berlin Heidelberg.

Dettman, J.W. 1965 *Applied complex variables*. Courier Corporation.

Hornbeck, R.W. 1964 Laminar flow in the entrance region of a pipe. *Appl. Sci. Res.* **13**, 224–232.

Khorrami, M.R., Malik, M.R. & Ash, R.L. 1989 Application of spectral collocation techniques to the stability of swirling flows. *J. Comp. Phys.* **81**, 206–229.

Leib, S.J., Wundrow, D.W. & Goldstein, M.E. 1999 Effect of free-stream turbulence and other vortical disturbances on a laminar boundary layer. *J. Fluid Mech.* **380**, 169–203.

Lewis, H.R. & Bellan, P.M. 1990 Physical constraints on the coefficients of Fourier expansion in cylindrical coordinates. *J. Math. Phys.* **31** (11), 2592–2596.

Tuckerman, L.S. 1989 Divergence-free velocity fields in nonperiodic geometries. *J. Comp. Phys.* **80** (2), 403–441.